Evidence for the "zigzag" model of the smectic-C phase in the liquid crystal 4'-butoxyphenylester 4-decyloxybenzoic acid (4OP10OB): A high-resolution x-ray study

Edward N. Keller, Ehud Nachaliel, and Dan Davidov
Racah Institute of Physics, Hebrew University, 91 904 Jerusalem, Israel

Christine Böffel
Max-Planck-Institut für Polymerforschung, D-6500 Mainz, West Germany
(Received 1 April 1986)

We report, for the first time to our knowledge, on high-resolution x-ray scattering measurements of the liquid crystal 4'-butoxyphenylester 4-decyloxybenzoic acid (4OP10OB) with emphasis on the smectic-C phase and the smectic-A to smectic-C phase transition. From angular scans in reciprocal space we found that the smectic-C layer planes undergo a continuous tilt ϕ_p with respect to temperature that can be described either by a Landau-type mean-field theory (which includes a sixth-order term in ϕ_p) or by a simple scaling form: $\phi_p \sim [(T_c - T)/T_c]^{0.44}$, where T_c is the smectic-A—smectic-C transition temperature. Simultaneous measurements of the lattice spacing in the smectic-C phase suggest that the molecules do not behave like rigid rods. We found that the diamagnetic part of the molecule strongly couples to the magnetic field and tilts independently of the aliphatic end chains. The end chains are melted and thus maintain an almost-temperature-independent contact angle to the layer planes. Our measurements are consistent with the "zigzag" model of Bartolino, Doucet, and Durand.

I. INTRODUCTION

The smectic-C phases of liquid crystals are characterized by a tilting of the molecules with respect to the smectic layers. The smectic-C phase and the nature of the smectic-A to smectic-C transition have been studied extensively both experimentally and theoretically during the last several decades and the reader is referred to the review of Goodby and Gray.[1] There has been renewed interest, recently, in smectic-C phases because the chiral-smectic-C phase (smectic-C^*) might exhibit ferroelectricity or antiferroelectricity.[2] However, there have been only a few studies of the smectic-C phase using high-resolution x-ray scattering such as the work of Safinya on the liquid crystal $\bar{8}$S5,[3] and mixtures of $\bar{8}$S5 and 4-(n-pentylphenylthio)-4'-(n-heptyloxy)benzoate ($\bar{7}$S5),[4] and Ocko *et al.* on N-4-(n-butyloxy)benzylidene-4'-(n-heptyl)aniline (4O.7).[5]

The measurements of Refs. 3, 4, and 5 have demonstrated that in the presence of a sufficiently strong magnetic field, the smectic-C phase is characterized by a ring of scattering in reciprocal space, consistent with the prediction of de Gennes.[6] The smectic-A to smectic-C phase transition was found to be a second-order transition with a continuous tilting of the molecules with temperature. Angular scans (called ϕ scans[7]) give two peaks, resulting from the intersection of the ring of scattering with the scattering plane. The angular positions of these peaks give the tilt angle, ϕ_p, which is the amplitude of the complex order parameter, as suggested by de Gennes.[6] Longitudinal scans in reciprocal space (approximately 2θ scans in real space) through these peaks yield the smectic-C layer spacing, d_C, which is smaller than the lattice spacing in the smectic-A phase, d_A. One can define a tilt angle, ϕ_x, from the measured layer spacing as follows,

$$\phi_x = \cos^{-1}(d_C/d_A) . \tag{1}$$

If the liquid crystal molecules are rigid rods, then $\phi_p = \phi_x$. Measurements of the liquid crystal 40.7 (Ref. 5) seem to suggest that, in fact, $\phi_p = \phi_x$. Results for 4-(n-pentylphenylthio)-4'-(n-octyloxy)benzoate ($\bar{8}$S5)[3] do not agree with such an equality. The need for further high-resolution x-ray studies on other materials was clear. In this context, we undertook a high-resolution x-ray scattering study of a new liquid crystal, 4'-butoxyphenylester 4-decyloxybenzoic acid (4OP10OB), with emphasis on the smectic-C phase and the smectic-A to smectic-C phase transition. This work is also a part of ongoing research on side-chain polymeric liquid crystals, and their associated monomeric liquid crystals. (At a later date, we plan to correlate our results for the smectic-C phase of 4OP10OB to the smectic-C phase of C-6 polysiloxane.[8]) Our results for the smectic-C phase of 4OP10OB *do* show a discrepancy between the tilt angle, ϕ_p as extracted from the angular scans, and the tilt angle, ϕ_x, calculated from Eq. (1).

Bartolino, Doucet, and Durand (BDD) have proposed a model to explain the disagreement between the optically measured tilt of the molecules and the molecular tilts calculated from x-ray measurements of the layer spacing.[9] BDD suggest that liquid crystal molecules, with long flexible side chains, take the shape of a "zigzag" within the smectic-C phase. The zigzag is composed of an aromatic rigid core that tilts with the layer planes somewhat independently of the flexible aliphatic end groups. On the other hand, the liquidlike end groups contact the layer planes with a temperature-independent angle.

A theory of Wulf[10] has also predicted an inequality between the measured layer tilt and the tilt calculated from the layer spacing. However, Wulf's theory can only be valid for those liquid crystals, such as 4OP10OB, for which the ϕ_p and ϕ_x are not equal.[10,3] On the other hand, the zigzag model can also explain the behavior of liquid crystals, such as 4O.7,[3] for which $\phi_p = \phi_x$ (this will be shown in Sec. IV).

This work is organized as follows. Section II describes our experimental apparatus and our samples. Section III gives an overview of the phases of 4OP10OB as identified by our high-resolution x-ray scattering measurements. In Sec. IV we discuss our results for the smectic-C phase, in the context of the zigzag model.

II. EXPERIMENTAL APPARATUS AND SAMPLE

The x-ray source used for these measurements is a 12 kW Rigaku rotating anode generator fitted with a copper anode. All measurements were done at the Cu $K\alpha_1$ wavelength of 1.541 Å, with the generator operating at 40 kV and 150 mA. Our precision ϕ-2θ goniometer is capable of an in-plane resolution of better than 1×10^{-4} Å^{-1} full width at half maximum (FWHM) at a typical scattering angle (2θ) of 3 deg. In fact, our use of germanium (111) crystals for the monochrometer and analyzer (in a nondispersive mode) in combination with vertical slits before and after the sample, gives us an in-plane resolution of 1×10^{-3} Å^{-1} (FWHM). In our experiments, the resolution of our setup in the direction vertical to the scattering plane is usually determined by the vertical angular acceptance of the analyzer crystal. This gives a vertical resolution of 0.14 Å^{-1} (FWHM). We can improve the vertical resolution to 0.03 Å^{-1} (FWHM) by the use of solar slits before and after the sample. In general, our x-ray setup is similar to that of Ref. 11.

The 4OP10OB sample was synthesized at the Institut für Polymerforschung in Mainz. Differential scanning calorimetry (DSC) measurements and polarization microscopy were used to identify tentatively the various phases and phase-transition temperatures of the sample (see Fig. 1). 4OP10OB's molecular structure is shown in Fig. 1.

For the x-ray measurements, approximately one x-ray absorption length of 4OP10OB was enclosed in a copper cell with beryllium windows. The sample cell sits on a temperature-controlled oven whose heating element consists of a thermoelectric heat pump. Our oven has a stability of 0.003 deg over a temperature range of -30 °C to 90 °C. The temperature of the sample is measured by a silicon diode to 0.01 °C and was calibrated by a thermocouple to an absolute temperature of 0.1 °C. A compact $SmCo_5$ permanent magnet provided an alignment field of 7.8 kG with a 6 mm gap. The magnet rests on the oven, surrounds the sample, and thereby acts as a heat shield for the sample. Altogether, our oven proved to be portable, compact, and highly versatile.

The typical procedure used to align the 4OP10OB sample was as follows: The temperature was raised to 361 K, past the isotropic-nematic phase transition, and allowed to remain at 354 K, in the nematic phase, for 2 h. From this point, the temperature of the sample could be lowered rapidly to the nematic—smectic-A phase transition (at 350 K) without adverse effects on the sample's alignment.

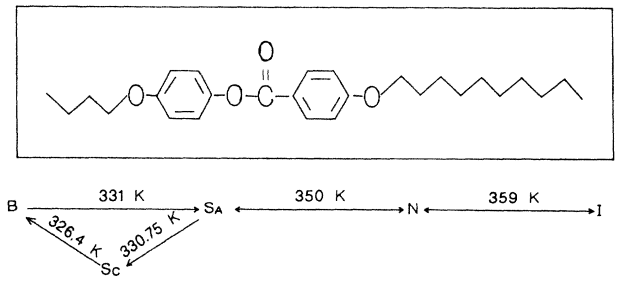

FIG. 1. Upper panel: Chemical formula of 4′-butoxyphenylester 4-decyloxybenzoic acid (4OP10OB). Lower panel: Phases and phase-transition temperatures for 4OP10OB as determined by DSC, polarization microscopy, and x-ray measurements.

III. X-RAY CHARACTERIZATION OF THE PHASES

The phases of 4OP10OB can be identified by 2θ scans across the peak of the scattering intensity in the scattering plane, as a function of temperature. Figure 2 summarizes the x-ray measurements of the scattering angle, 2θ, through much of the smectic range of 4OP10OB. The layer thickness, d, can be calculated from 2θ by the Bragg equation,

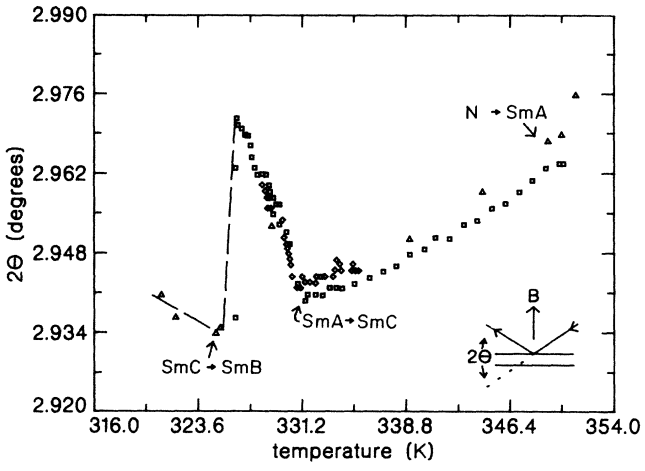

FIG. 2. Measurement of the peak position (2θ) as a function of temperature (K) (the scattering configuration is shown on the lower right-hand side). The arrows indicate the various phase transitions: nematic to smectic-A ($N\rightarrow$SmA), smectic-A to smectic-C phase (Sm$A\rightarrow$SmC), and smectic-C to smectic-B (Sm$C\rightarrow$SmB) phase transitions. The squares, □, triangles, △, and diamonds, ◇, represent separate measurements. The ◇ measurements are the most accurate and have been used for all the calculations in this work. The dashed line is a guide to the eye. The 2θ values yield the layer spacings with use of Eq. (2).

$$d=(\lambda/2)/\sin(2\theta/2)\,, \tag{2}$$

where 2θ is taken at the peak of the scan (see Fig. 3) and λ is the wavelength of the x rays (1.541 Å). The variations between the different measurements overplotted in Fig. 2 are probably due to different levels of contaminants that shift the transition temperature, but do not seem to affect the nature of the phase transitions.[12] The set of closely spaced measurements, in Fig. 2, were the most precise ones performed and will be used for all the quantitative results of this work. Note that the transition temperatures, appearing as cusps, are well characterized by the x-ray results in Fig. 2. We were able to identify the nematic, smectic-A and smectic-C phases by our x-ray measurements. Details are given below. The lowest temperature phase was identified by polarization microscopy to be smectic-B phase. No x-ray work was done to independently verify the indentity of this phase.

A. Smectic-A phase

Our measurements of the nematic—smectic-A phase transition at 350 K revealed no pretransition effects. The McMillan ratio,[13] T_{NA}/T_{NI}, for this transition was 0.97.

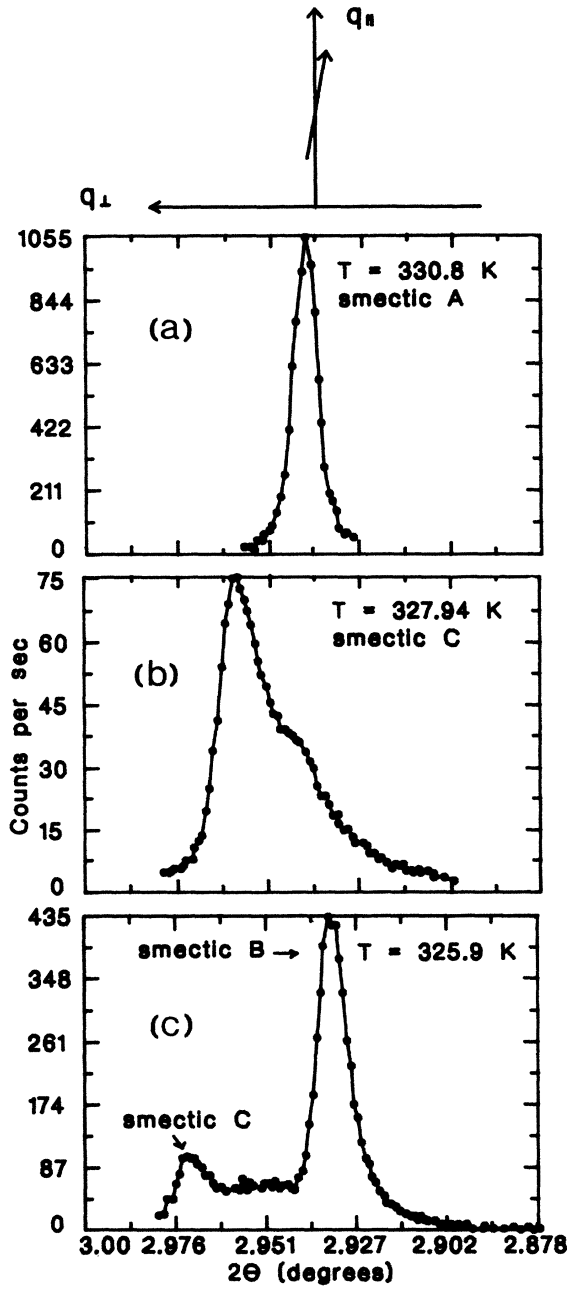

FIG. 3. Upper panel: Trajectory of a 2θ scan in reciprocal space. Lower panels: (a) 2θ scan of the smectic-A phase at 330.8 K and $\phi=0°$. (b) 2θ scan of the smectic-C phase at 327.94 K and $\phi=-8°$. (c) 2θ scan of the coexistence of smectic-C and smectic-B phases at 325.9 K and $\phi=0°$. The solid lines are a guide to the eye.

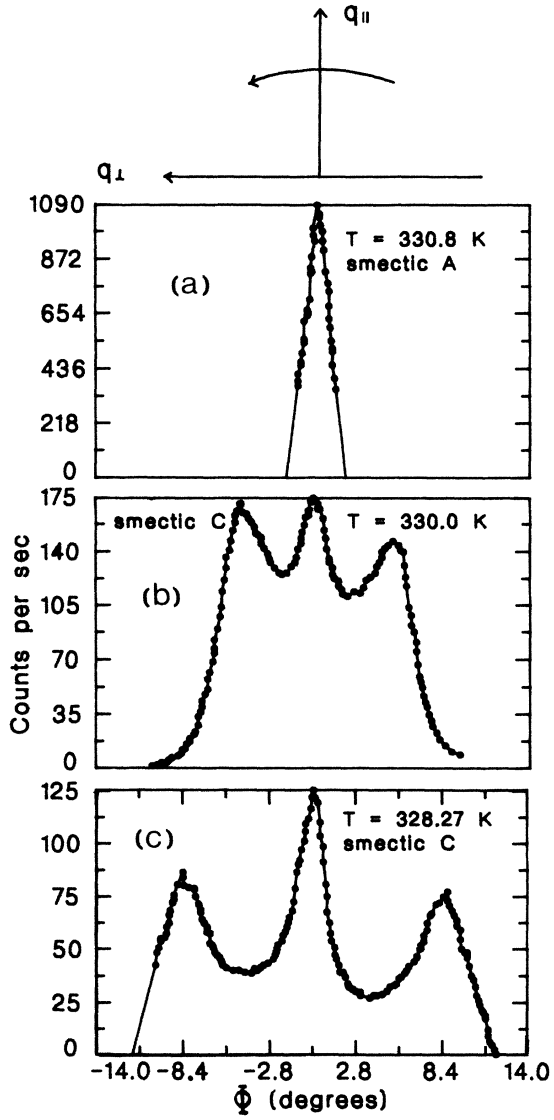

FIG. 4. Upper panel: Trajectory of a phi scan in reciprocal space. Lower panels: (a) phi scan of the smectic-A phase at 330.8 K, and $2\theta=2.942°$; (b) phi scan of the smectic-C phase at 330.0 K, and $2\theta=2.950°$; (c) phi scan of the smectic-C phase at 328.27 K, and $2\theta=2.960°$. The solid lines are a guide to the eye.

These measurements are consistent with a first-order phase transition. Figure 3(a) displays the results of a 2θ scan (roughly equivalent to a longitudinal scan in q space) just before the phase transition to the smectic-C phase. The FWHM of the 2θ scan in Fig. 3(a) is 0.008 deg (1.1×10^{-3} Å^{-1}), so it is essentially resolution limited. We also measured the 2θ scan of the harmonic, which gave a peak at exactly twice the scattering angle of the fundamental. Figure 4(a) shows the results of a phi scan (angular scan in q space) at the same temperature. Altogether, the pattern of the 2θ, harmonic, and phi scans is consistent with the smectic-A phase (see, for example, Ref. 3).

B. Smectic-C phase

Figures 4(b) and 4(c) show the results of phi scans within the smectic-C phase. The peaks on both sides of $\phi=0$ correspond to the intersection of the broadened ring of scattering with the scattering plane. As can be clearly seen, the splitting between these peaks increases with decreasing temperature below the smectic-A–smectic-C phase transition [Figs. 4(b) and 4(c)]. This splitting yields $2\phi_p$ directly. The central peak [Figs. 4(b) and 4(c)] is generally referred to as a pinned smectic-C phase.[3] In the pinned smectic-C phase, wall effects can contribute to the free energy in such a way as to make tilting of the molecules energetically favorable to tilting of the planes. Figure 3(b) shows a 2θ scan deep within the smectic-C phase (at 327.94 K). The 2θ scan was measured at one of the peaks of the phi scan ($\phi=-8°$). The long tail in the direction of small 2θ is caused by scattering from planes tilted with respect to the plane of the magnet, as discussed below.

Two-dimensional q scans were performed in order to obtain a more global picture of the scattering. Figure 5 shows the fourth quadrant of the scattering plane in reciprocal space at two temperatures in the smectic-C phase. The slow rise in intensity, along radii radiating from the origin of q space, corresponds to the 2θ scan tail of Fig. 3(b). The peak near $q_\perp=0$ corresponds to the pinned smectic-C peaks of Figs. 4(b) and 4(c). The peak intensities, in Fig. 5, follow a circle in reciprocal space. The circular pattern is produced by mosaics of the same layer thickness, but whose layers are tilted along a range of angles, $\phi_p\geq\phi\geq0$. Since the smectic-C phase is characterized by cylindrical symmetry about the direction of the magnetic field ($\phi=0$), these mosaics broaden the ring of scattering of the smectic-C phase into a solid cone in reciprocal space. The projection of the cone onto the scattering plane is a crescent.

We also measured 2θ scans at phi coordinates corresponding to the pinned smectic-C peak ($\phi=0$). At these points, the contribution to the total scattering intensity from mosaics, above and below the scattering plane, is much smaller. This was in fact observed; the typical FWHM of these 2θ scans are 0.008 deg (1.1×10^{-3} Å^{-1}) and are resolution limited. Nevertheless, the peak position of the 2θ scan of the pinned smectic-C peak was the same as the 2θ peak position of the nonpinned peak. This shows that the 2θ scan's peak position is not affected by the mosaics in the sample. Therefore, we are confident that the layer spacing can be calculated from the peak position of the 2θ scans, without detailed deconvolution analyses.

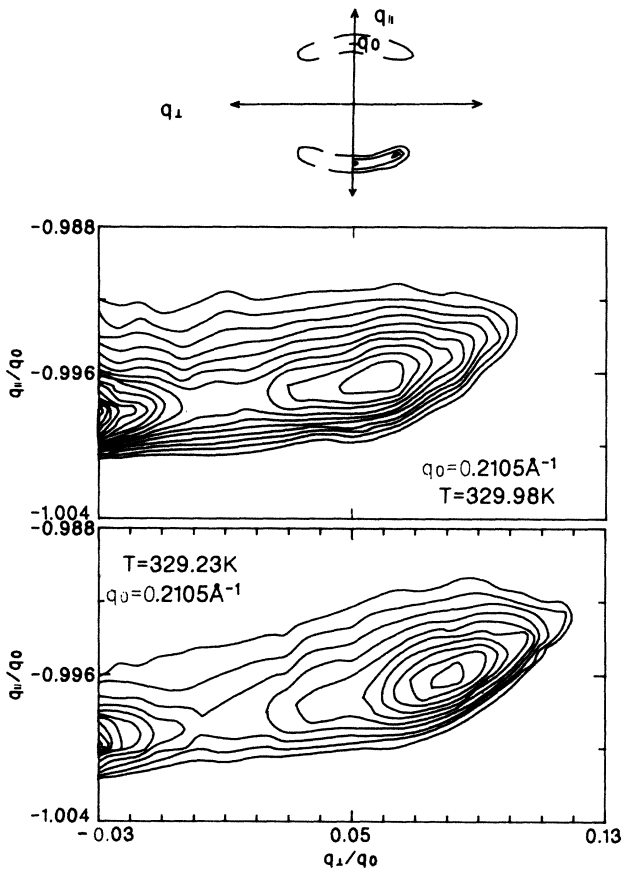

FIG. 5. Upper panel: Overview of in-plane scattering for the smectic-C phase. Center panel: the measured scattering in the fourth quadrant of the scattering plane at 329.98 K. Lower panel: The measured scattering in the fourth quadrant of the scattering plane at 329.23 K. Contours correspond to lines of equal intensity.

C. Smectic-B phase

Figure 3(c) shows a 2θ scan right at the smectic-C–smectic-B transition. The two peaks in Fig. 3(c) show that there is a coexistence region for the smectic-C and smectic-B phases. A smectic-B–smectic-C coexistence region was also measured by Ocko *et al.* for N-4(*n*-butyloxy)benzylidene-4-(*n*-heptyl)aniline (4O.7).[5] The coexistence region in 4OP10OB is approximately 0.5 K wide. The rapid collapse of the smectic-C phase suggests that the smectic-C to smectic-B transition is, mainly, first order.

IV. DISCUSSION

Figure 6 plots the layer tilt, ϕ_p, measured from the phi scans as a function of temperature. Like Ocko,[5] we have fitted this behavior to a Landau-type mean-field model

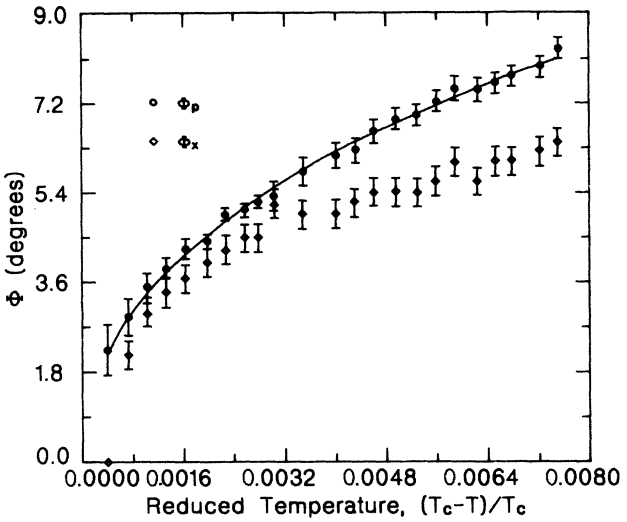

FIG. 6. Plots of the tilt angle, ϕ_p, measured from the phi scans, and the tilt angle, ϕ_x, calculated from the measured layer spacings [using Eq. (1)] as a function of reduced temperature. The solid line is a fit to Eq. (3) with $T_c=330.75$ K and $t_0=0.0049$.

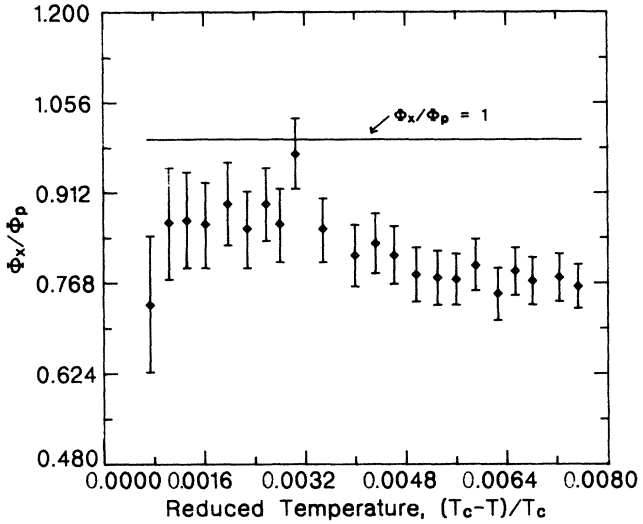

FIG. 7. The ratio, ϕ_x/ϕ_p, as a function of the reduced temperature. The rigid rod limit, $\phi_x/\phi_p=1$, is shown by the solid line.

that includes a sixth-order term in ϕ_p. This gives[5]

$$\phi_p \sim [(1+t/t_0)^{1/2}-1]^{1/2}, \tag{3}$$

where t is the reduced temperature, $(T-T_c)/T_c$, and t_0 is a crossover temperature at which the order parameter begins to saturate.[5] Excellent fits were found for $T_c=330.75\pm0.04$ K and for $0.0049\leq t_0\leq 0.0075$. The fitted value of T_c is consistent with the measurements shown in Fig. 2, and indicates that the smectic-A to smectic-C transition is second order up to $t=0.0075$. The solid line in Fig. 6 is a fit to Eq. (3) with $T_c=330.75$ K and $t_0=0.0049$. The tilt, ϕ_p, can also be fitted to a simple scaling form,

$$\phi_p=\phi_0 t^{\beta} \tag{4}$$

then the critical exponent, β, obtained is $\beta=0.44\pm0.02$. We have no *a priori* reason to prefer Eq. (3) over Eq. (4), since both give equally excellent fits to the data. Figure 6 also plots the tilt angle, ϕ_x, as calculated from the measured lattice spacings, d_c, using Eq. (1) with d_A equal to the measured spacing at the smectic-A to smectic-C transition (30.014 Å). As clearly seen, there is a significant discrepancy between the measured tilt, ϕ_p, and the tilt, ϕ_x, calculated from the layer spacing. The ratio ϕ_x/ϕ_p is plotted as a function of reduced temperature in Fig. 7. If the 4OP10OB molecules were rigid rods, ϕ_x/ϕ_p would be equal to 1 (solid line in Fig. 7).

Following the model of Bartolino, Doucet, and Durand,[9] we assume that the 4OP10OB molecule can be subdivided at the terminal oxygens into a rigid core and two flexible end chains (see Fig. 8). Using the notation of Ref. 9, we denote the length of the aromatic core by a_0, and the length of the two end chains at the smectic-A–smectic-C transition, by l_1 and l_2. Since the rigid core is diamagnetic, it aligns with the magnetic field and tilts with an angle ϕ_p to the layer planes. ϕ_p is also the measured tilt angle of the layers with respect to the magnetic field direction. Assuming that the aliphatic groups can pivot at the terminal oxygens and make an angle Ω with the layer planes, (as shown in Fig. 8), then the measured layer thickness, d_c, is related to a_0, l_1, and l_2 by,

$$d_c=a_0\cos(\phi_p)+(l_1+l_2)\cos(\Omega)\,. \tag{5}$$

Note that this model is independent of molecular rotation. If the molecules rotate, then the layer spacing is determined by the total volume swept out during a rotation, giving the same d_c as in Eq. (5). We have no independent absolute measurement of a_0 and l_1 and l_2. To calculate

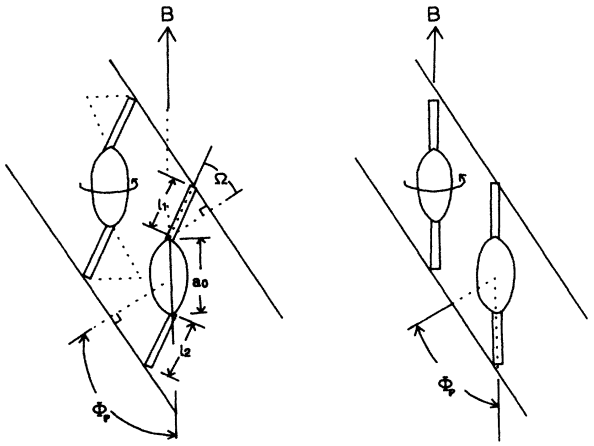

FIG. 8. Left panel: The zigzag model for the smectic-C phase. The diamagnetic cores of length, a_0, align with the magnetic field at an angle ϕ_p to the layer planes, while the flexible chains of lengths l_1 and l_2 contact the layer planes at an angle Ω. Notice that molecular rotations do not change the layer spacing. Right panel: The rigid rod model for the smectic-C phase. The entire molecular aligns with the magnetic field which is at an angle ϕ_p to the layer planes.

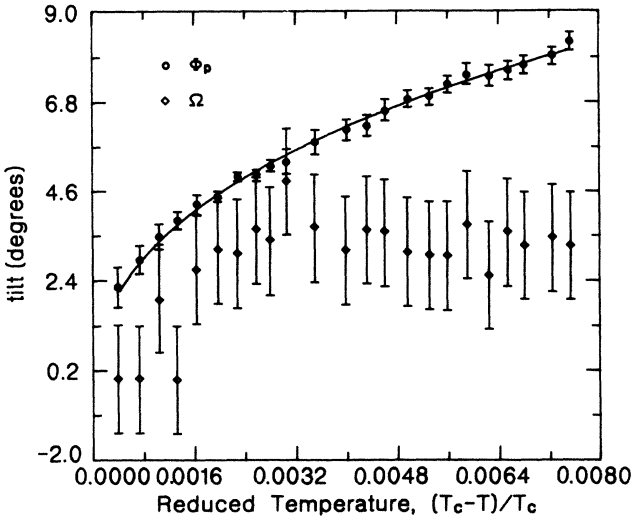

FIG. 9. A plot of the tilt angle, ϕ_p, of the molecule's diamagnetic core, and a plot of the tilt angle, Ω, of the aliphatic chains as a function of reduced temperature. The solid line indicates a fit to Eq. (3) with $T_c = 330.75$ K and $t_0 = 0.0049$.

Ω, we have used the value of a_0 calculated in Ref. 9 for 4'-butoxyphenylester 4-nanyloxybenzoic acid (4OP9OB). $l_1 + l_2$ can then be determined by subtracting a_0 from the measured length of the molecule, d_A, at the smectic-A–smectic-C transition. This gives $a_0 = 14.8$ Å and $(l_1 + l_2) = 15.2$ Å. Figure 9 shows the calculated value of Ω along with the measured tilt angle, ϕ_p. For $t \geq 0.002$, Ω is constant with a value of ~ 3.4 deg. This behavior is not surprising if the aliphatic chains are melted, as originally suggested by Guillon and Skoulios.[14] It is possible, in such a case, that the end chains will maintain a stable configuration, with respect to the layer planes, that is independent of the aromatic core's tilt.

Finally, BDD (Ref. 9) have defined a ratio, $\alpha = a_0/L$, between the calculated length of the rigid part of the molecule, a_0, and the calculated all-extended all-trans length of the molecule, L. The parameter α measures the rigidity of the molecules; the larger the α the closer the molecule is to a rigid rod. We expect a trend to emerge, viz., as the α approaches 1, then the ratio ϕ_x/ϕ_p should approach the rigid rod limit of 1.

To compare materials, it is necessary to compute a temperature-independent ratio, r, that is related to ϕ_x/ϕ_p. We see from Eq. (3), that ϕ_p^2 will have a constant slope for $t < t_0$. ϕ_x^2 will have a constant slope for $t_1 \leq t < t_0$, where t_1 is the temperature above which Ω is constant. We have therefore calculated (following Ref. 9) the ratio, r^2, of the slopes of ϕ_x^2 and ϕ_p^2, for temperatures in the range $t_1 \leq t < t_0$. In the case of 4OP10OB, the appropriate range for calculating r^2 is $0.002 \leq t < 0.0075$. (For the materials of Refs. 3, 4, 5, and 9, t_1 appears to be approximately 0.) In Table I, we have compiled the results of BDD (Ref. 9) for α and r with our results. We have also included, in Table I, the values of α and r calculated using the data of Ocko *et al.*,[5] and Safinya *et al.*[3] The general tendency in Table I suggests that there is a correlation between the rigidity parameter α and the ratio $r \sim \phi_x/\phi_p$, as expected for the zigzag model.

TABLE I. Correlation between the rigidity parameter, α, and the ratio r ($r = [\text{slope}(\phi_x^2)/\text{slope}(\phi_p^2)]^{1/2}$).

Material	L (Å)	a_0 (Å)	$\alpha = a_0/L$	r
AMC11[b]	49	18.0	0.37	0.50
4OP10OB[a]	31.2	14.8	0.47	0.63±0.04
4OP9OB[b]	30	14.8	0.49	0.67
70.7[b]	30.4	15.4	0.51	0.72
$\bar{8}$S5[c]	29.4	15.6	0.53	0.70
40.7[d]	26.7	15.4	0.58	1.0
TBBA[b]	28.6	25.0	0.87	0.93

[a]This work.
[b]Reference 9.
[c]Reference 3.
[d]Reference 5.

In conclusion, the zigzag model can adequately explain the "discrepancy" between ϕ_x and ϕ_p. This model suggests that the aliphatic end chains are melted and the forces responsible for the molecular tilts *originate in the aromatic cores.* Previous evidence for the zigzag model was based on less precise x-ray and optical work. High-resolution x-ray measurements add much credence to this model. More work is needed in this field. A study of the deuterated end chains, using NMR, could be especially useful.

ACKNOWLEDGMENTS

We would like to thank Dr. Marcel Bretschneider for writing many of the computer programs that drive our equipment, and Dr. Moshe Deutsch for providing us with the germanium crystals used in our spectrometer. We gratefully acknowledge stimulating discussions with Professor S. Alexander, Professor Z. Luz, and Professor H.W. Spiess. This work has been supported by the National Council for Research and Development, Israel, and the Kernforschungsanlage Jülich, Germany.

[1]J. W. G. Goodby and G. W. Gray, *Smectic Liquid Crystals* (Leonard Hill, Glasgow, 1984).
[2]S. Dumiongrattana and C. C. Huang, Phys. Rev. Lett. **56**, 464 (1986).
[3]C. R. Safinya, M. Kaplan, J. Als-Nielsen, R. J. Birgeneau, D. Davidov, J. D. Litster, D. L. Johnson, and M. E. Neubert, Phys. Rev. B **21**, 4149 (1980).
[4]C. R. Safinya, Ph.D. thesis, M.I.T., 1981.
[5]B. M. Ocko, A. R. Kortan, and R. J. Birgeneau, J. Phys. (Paris) **45**, 113 (1984).
[6]P. G. de Gennes, Mol. Cryst. Liq. Cryst. **21**, 49 (1973).
[7]M. C. Kaplan, Ph.D. thesis, M.I.T., 1980.
[8]E. Nachaliel, E. N. Keller, D. Davidov, H. Zimmermann, and M. Deutsch, in proceedings of the International Conference

on Liquid Crystals, Berkeley, California, 1986 (unpublished).
[9]R. Bartolino, J. Doucet, and G. Durand, Ann. Phys. (Paris), 3, 389 (1978).
[10]A. Wulf, Mol. Cryst. Liq. Cryst. 56, 123 (1979).
[11]J. Als-Nielsen, R. J. Birgeneau, M. C. Kaplan, J. D. Litster, and C. R. Safinya, Phys. Rev. Lett. 39, 352 (1977).
[12]B. M. Ocko, Ph.D. thesis, M.I.T., 1984, p. 110.
[13]W. McMillan, Phys. Rev. A 4, 1238 (1971).
[14]D. Guillon and A. Skoulios, J. Phys. (Paris) 38, 79 (1977).